

performance and compared with JPEG. Rafeef Abugharbieh et al [2] presented a novel 3-D scalable compression method for medical images with optimized volume of interest (VOI) coding. A new technique of 3D wavelet transform was proposed by Gregorio Bernabe et al [3] for medical videos. Here a lossy compression technique was used which was on the basis of the 3D fast wavelet transform especially for encoding the medical videos. Yen-Yu Chen et al [4] has designed a novel medical image compression technique. In this method, high-frequency sub bands are used in good number for reducing the redundancy by promoting the algorithm with modified SPIHT. Srikanth et al [5] has put forth a method for medical image compression, this paper focused mainly on the lossless coding of the images, and then compares the performance of both the uniform and adaptive mesh-based methods. Shyam Sunder et al [6] have jointly framed a novel medical image compression technique by using 3-D Hartley transform. Aaron et al [7] have proposed a method called lossless image compression with projection-based and adaptive reversible integer wavelet transforms. Harjeetpal Singh et al [8] presented a hybrid model which is the combination of several compression techniques. This paper presents DWT and DCT implementation because these are the lossy techniques and also introduce Huffman encoding technique. The results show that the proposed hybrid algorithm performs much better in term of peak-signal-to-noise ratio with a higher compression ratio compared to standalone DCT and DWT algorithms. David Wu et al [9] proposed a coder which outperformed the LOCO coder while preserving the visual fidelity of the image the heart of the proposed coder. Sivanantha Raja et al [10] described a novel approach to medical image compression using the Curvelet Transform. This method gives higher compression ratio compared other compression schemes proposed earlier. Marykutty Cyriac et al [11] proposed a method in which, the run length is stored in the pixel value itself for single run pixels thus reducing the size of the encoded vector. Visually lossless compression with high PSNR value is obtained. M.Ferni Ukrit et al [12] performed a survey on various lossless compressing techniques. Aleksej Avramovic et al [13] described predictive lossless image compression process. Mrs.S.Sridevi et al [14] reviewed various medical image compression techniques such as JPEG2000, JPEG2000 scaling based ROI coding, JPEG2000 MAXSHIFT ROI coding, Shape Adaptive wavelet transform and scaling based ROI, Discrete cosine transform, Discrete wavelet transform, Mesh based coding scheme, Sub band block hierarchical partitioning. Balpreet Kaur et al [15] proposed the ROI is compressed with lossless and lossy techniques. Pasumpon Pandian et al [16] proposed a new hybrid image coding algorithm based on a sequencing that is simple to cast and encode the bit planes. Zixiang Xiong et al [17] have jointly proposed a technique called lossy to lossless compression using 3D wavelet transforms. Ramakrishna et al [18] has developed a medical image compression technique called internet transmission of DICOM images with effective low bandwidth utilization. 3-D medical image compression using 3-D wavelet coders was developed by Sriraam et al [19], Janaki et al [20] proposed a technique for image compression which uses the Wavelet-based Image Coding in combination

with Huffman encoder for further compression. Avidan et al [21] presented a novel content-aware image resizing method based on wavelet analysis is to estimate the local energy map of an image by weighing its multi scale sub bands appropriately. Based on the energy map, the image is resized by repeatedly carving out or inserting in a connected path of pixels, which is least significant in terms of the energy. It is an emerging image resizing paradigm. For Seam carving, the importance of pixels is defined by an energy function and based upon this function; the image size can be changed by gracefully carving-out or inserting pixels in different parts of the image. Calculate forward and backward energy and then forward energy can achieve better retargeting performance. Here, the experiments conducted to evaluate the spatial-scalability and compression performance of the proposed seam energy based SPIHT codec. Gutierrez et al [22] proposed the comprehensive perceptual study and analysis of image retargeting. First, create a benchmark of images and conduct a large scale user study to compare a representative number of state-of-the-art retargeting methods. In order to balance the visual quality of retargeted image and the coding efficiency, the wavelet decomposition scale is fixed as two, and, accordingly, each seam in the low-frequency sub band reflects four neighbouring columns or rows in the image domain. Hasegawa et al [23] presented image resizing technique which shrinks an image size but does not change important region(s) in the original image, whereas image dilution is the reverse process to image concentration. An image retargeting method called seam carving is used for image concentration. The image concentration (dilution) is a pre (post)- processing of image encoder (decoder). In the experimental results, JPEG/SPIHT with image concentration/dilution presents significant bit rate savings compared with the original JPEG/SPIHT alone and reconstructed image qualities are very similar to each other. The objective of this system is to provide high compression ratio with better quality in medicines. This paper aims to integrate lossy and lossless compression method for reducing redundancy in medical images. The remainder of this paper is organized as follows. Section 2 introduces the proposed image coding scheme in detail, including block-based seam energy map generation, Integer wavelet transform, SPIHT and arithmetic encoding, Section 3 demonstrates the simulation results compared with other relevant state-of-the-art image coding schemes, while Section 4 concludes this paper.

2 PROPOSED METHOD

An approach has been made to build the integrated system for medical image compression. The block diagram of proposed method is shown in figure 1b. The system consists of two major parts. The first part is the removal of noisy pixel in an image using seam carving and energy mapping. The second part of the system is to perform compression using integer wavelet transform followed by SPIHT, arithmetic coding. Furthermore, the proposed method is analyzed with PSNR and compression rate. It also significantly reduces the computational time for

compression and decompression

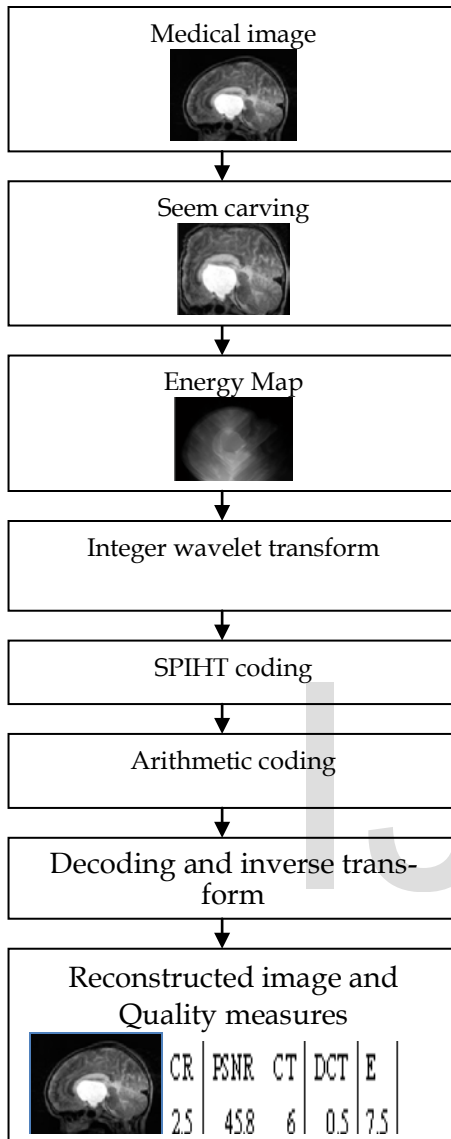


Figure1b: Block Diagram of Proposed method

2.1 Seam Carving For Image Retargeting

A seam is defined as a continuous path of pixels running from the top to the bottom of an image in the case of a vertical seam, while a horizontal seam is a continuous line of pixels spanning from left to right in an image. The process allows the user to resize an image by removing a continuous path of pixels (a seam) vertically or horizontally from an image.

2.1.1 Algorithm implementation

Step 1: Read the input image

Step 2: Calculate the weight / density / energy of each pixel. This can be done by various algorithms: gradient magnitude,

entropy, visual saliency, eye-gaze movement. Figure 2 is gradient image of an input image. The sobel operator was chosen for calculation of the gradient image, but other gradient operators may be used.

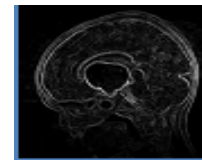


Figure 2: Gradient Image

Step 3: Once the gradient image is calculated, the next step is to calculate the energy map image

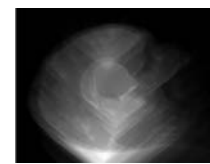


Figure 3: Seam Energy map

It is shown in Figure 4.12b, the energy map image needs to be calculated separately for either vertical or horizontal seams, Seams are ranked by energy, with low energy seams being of least importance to the content of the image

Dynamic programming is used in seam carving for computing seams. If attempting to compute a vertical seam (path) of lowest energy, for each pixel in a row we compute the energy of the current pixel plus the energy of one of the three possible pixels above it. This is better described by figure 4.

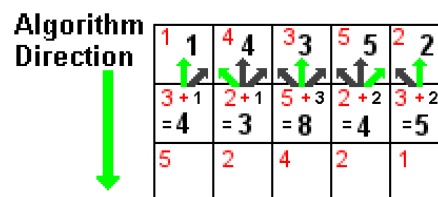


Figure: 4 Computation of seams

Each square represents a pixel, with the top-left value in red representing the energy value of that said pixel. The value in black represents the cumulative sum of energies leading up to and including that pixel. The first row has no rows above it, so the sum (black) is just the energy value of the current pixel (red). The second row, if we look at the second pixel for example, we see its energy value is 2 (red). If we look above it, it has a choice of 1, 4, or 3 (black). Since 1 is the minimum number of the three values, we ignore the other two and set the sum of the pixel to its energy value which is 2 (red) plus 1 (black). After the above operation is carried out for every pixel in the second row, we go to the third row. We repeat the process to trace the seam/path. A cost function with a Lagrange multiplier is utilized, and it is formulized as follows:

$$CF = \text{Argmin} \{E_B(S_B) + \lambda R_B(S_B)\} \quad (1)$$

where $S_B = 2^L \times 2^L$ denotes the width and height in seam unit of the block-based vertical seam, is the optimized block size, and E_B and R_B are the average forward seam energy induced by removing a block based vertical seam and the required bit stream to transmit the pixel value (or transformed coefficients) and side information of the seams. For an $N \times M$ original image, E_B and R_B can be calculated as

$$E_B(S_B) = \sum_J M_B(N/2^L, j) / (M/2^L) \quad (2)$$

$$R_B(S_B) = R_c(S_B) + R_s(S_B) \quad (3)$$

Where $M_B(N/2^L, j)$ represents the last row of the cost matrix M_B in, J is the column index and $J \in [0, M/2^L]$; $R_c(S_B)$ and $R_s(S_B)$ are the coded bits generated by encoding the wavelet coefficients and the position information of the corresponding seam paths, respectively. For the vertical seams, each entry in M_B is updated by

$$M_B(i/2^L, j/2^L) = W(i/2^L, j/2^L) + \min \{M_B((i-2^L)/2^L, (j-2^L)/2^L) + C_L^B \{M_B((i-2^L)/2^L, (j)/2^L) + C_U^B \{M_B((i-2^L)/2^L, (j+2^L)/2^L) + C_R^B \quad (4)$$

where C_L^B, C_U^B, C_R^B are the costs for the three possible connection paths of a block-based vertical seam. $W(\cdot)$ is a weighting parameter that can be used to balance seam removal/insertion

$$C_L^B = \sum_{k=j}^{i+j-1} |I(k, j+2^L) - I(k, j-1)| + \sum_{k=j}^{i+j-1} |I(i-1, k) - I(i, k+2^L)| \quad (5)$$

Step 4: Then remove the seams from the image, reducing the size of the image.

2.2 Integer wavelet Transform

Recently, wavelets [23] have been used frequently in medical image processing. The biorthogonal wavelet transform is taken in this method because it is symmetric, almost orthogonal and gives the best results for medical images. The image is decomposed into different frequency components. It is performed by applying 1-D DWT along the rows of the image first, and then, the results are decomposed along the columns. The following sequence of operations is done for performing Lifting:

1. Split S_j into Even_{j-1} and Odd_{j-1}
2. $d_{j-1} = \text{Odd}_{j-1} - \text{Predict}(\text{Even}_{j-1})$
3. $S_{j-1} = \text{Even}_{j-1} + \text{Update}(d_{j-1})$

The Fig 5 shows the forward transform visually.

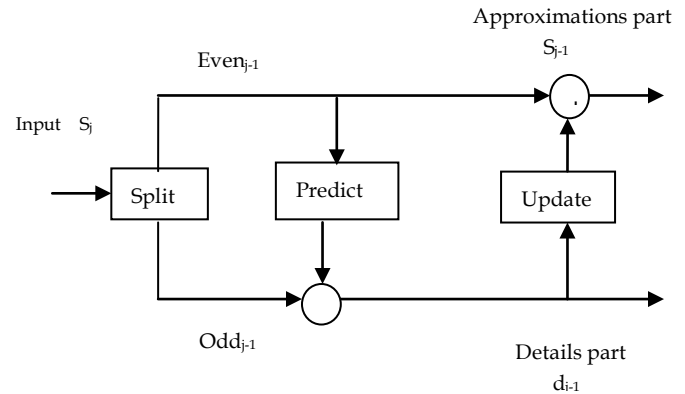


Figure 5-Block diagram of forward transform

The lifting approach [24] allows fast, efficient, and in-place calculation of the wavelet transform. Applying wavelet transform to S_j divides it into coarse S_{j-1} values and detail d_{j-1} values. Two operations are used for performing the lifting transform. They are Predict and Update.

Lifting step is the operation of obtaining the differences from the prediction. After the prediction step, the update step is followed. In the update step, the even values are updated and the odd samples become the scaling coefficients. These scaling coefficients pass on to the next stage of transform. Finally the odd elements are replaced by the difference and the even elements by the averages. The computations in the lifting scheme are done in place which saves lot of memory and computation time. The lifting scheme provides integer coefficients and so it is exactly reversible.

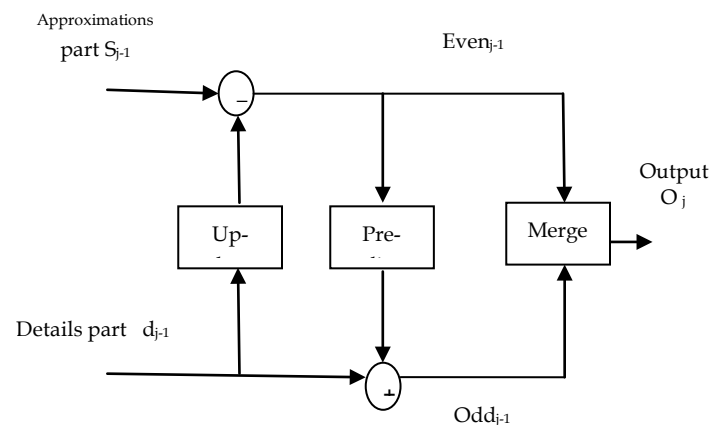


Figure 6-Block diagram of inverse transform

The Fig 6 shows the inverse transform visually. The inverse operation is done by performing the following sequence of operations:

1. $\text{Even}_{j-1} = S_{j-1} + \text{Update}(d_{j-1})$
2. $\text{Odd}_{j-1} = d_{j-1} + \text{Predict}(\text{Even}_{j-1})$
3. $O_j = S_j = \text{Merge}(\text{Even}_{j-1}, \text{Odd}_{j-1})$

The original signal is retrieved back by the inverse transform by reversing the operations of the forward transform and replacing the split operation with a merge operation. The lifting process provides spatial de-correlation of image data.

2.3 Set Partitioning In hierarchal Trees

SPIHT (Singh et al 2012) is a medical image coder that exploits the inherent similarities across the sub bands in an integer wavelet decomposition of an image. The SPIHT (Set Partitioning in Hierarchical Trees) algorithm is a fast and efficient technique for image compression and encryption. SPIHT generally operates on an entire image at once. The method deserves special attention because it provides the advantages like highest image quality, progressive image transmission, fully embedded code file, simple quantization algorithm, fast coding/decoding, completely adaptive, lossless compression, exact bit rate coding and error protection. In the SPIHT algorithm, the image is first decomposed into a number of sub bands by means of hierarchical wavelet decomposition. The sub band coefficients are then grouped into sets known as spatial-orientation trees, which efficiently exploit the correlation between the frequency bands. The coefficients in each spatial orientation tree are then progressively coded from the most significant bit-planes (MSB) to the least significant bit-planes (LSB), starting with the coefficients with the highest magnitude and at the lowest pyramid levels.

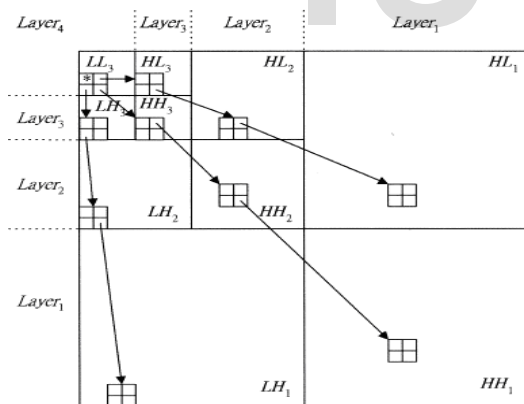


Figure 7: Structure of SPIHT encoding method

The original image is decomposed into sixteen sub bands which are shown in Fig 7. The SPIHT multistage encoding process employs three lists and sets: SPIHT has 3 lists

- LIP: list of insignificant pixels (individual insignificant coefficients)
- LIS: list of insignificant lists (insignificant trees)

- LSP: list of significant pixels (significant coefficients)
- SPIHT defines 2 types of trees
- Type M: check all descendants for significance
 - Type P: check all descendants except immediate children

Step 1: Initialization

Compute initial threshold

LIP: all root nodes (in low pass sub band)

LIS: all trees (type M)

LSP: empty

Step 2: Sorting Pass

Check significance of all coefficients in LIP:

If significant, output 1 followed by a sign bit & move it to LSP.

If insignificant, output 0.

Step 3: Check significance of all trees in LIS

For type-M tree:

If significant, output 1 & proceed to code its children

If a child is significant, output 1, sign bit, & add it to LSP.

If a child is insignificant, output 0 and add it to the end of LIP.

If the child has descendants, move the tree to the end of LIS as type L, otherwise remove it from LIS.

If insignificant, output 0.

For type-P tree :

If significant, output 1, add each of the children to the end of LIS as type M and remove the parent tree from LIS.

If insignificant, output 0.

Step 4: Refinement pass

For each element in LSP – except those just added above, output the nth most significant bit of coefficient.

End loop over LSP.

Step 5: Decrease the threshold by a factor of 2. Go to Step 2.

The rate can be controlled by using this algorithm. Till the desired distortion value is reached, the encoder continues estimating the progressive distortion reduction. The same number of lists is replicated by the SPIHT decoder algorithm and also the ordering information is recovered easily.

2.4 Adaptive Arithmetic Encoder

It is the method of representing frequently occurring pixel values into fewer bits. In arithmetic coding (suneetha et al 2007), single codes are used to represent a string of character thereby reducing the file size. Arithmetic coding is a form

of variable-length entropy encoding used in lossless data compression. Normally, a string of characters such as the words "hello there" is represented using a fixed number of bits per character, as in the ASCII code. When a string is converted to arithmetic encoding, frequently used characters will be stored with fewer bits and not-so-frequently occurring characters will be stored with more bits, resulting in fewer bits used in total. Arithmetic coding differs from other forms of entropy encoding such as Huffman coding in that rather than separating the input into component symbols and replacing each with a code, arithmetic coding encodes the entire message into a single number, a fraction n where $(0.0 \leq n < 1.0)$. In arithmetic coding, a message is encoded as a real number in an interval from one to zero. Arithmetic coding typically has a better compression ratio than Huffman coding, as it produces a single symbol rather than several separate codeword's. Arithmetic coding is a lossless coding technique. There are a few disadvantages of arithmetic coding. One is that the whole codeword must be received to start decoding the symbols, and if there is a corrupt bit in the codeword, the entire message could become corrupt. Another is that there is a limit to the precision of the number which can be encoded, thus limiting the number of symbols to encode within a codeword. There also exist many patents upon arithmetic coding, so the use of some of the algorithms also call upon royalty fees. Here is the arithmetic coding algorithm, with an example to aid understanding.

Step 1: Start with an interval $[0, 1)$, divided into subintervals of all possible symbols to appear within a message. Make the size of each subinterval proportional to the frequency at which it appears in the message. Eg:

Table 1 calculation of cumulative probability

Symbol	Probability	Interval
a	0.2	$[0.0, 0.2)$
b	0.3	$[0.2, 0.5)$
c	0.1	$[0.5, 0.6)$
d	0.4	$[0.6, 1.0)$

Step 2: When encoding a symbol, "zoom" into the current interval, and divide it into subintervals like in step one with the new range. Example: suppose we want to encode "abd". We "zoom" into the interval corresponding to "a", and divide up that interval into smaller subintervals like before. We now use this new interval as the basis of the next symbol encoding step.

Table 2 calculation of new cumulative probability after symbol "a" has occurred

Symbol	New "a" Interval
a	$[0.0, 0.04)$
b	$[0.04, 0.1)$
c	$[0.1, 0.102)$
d	$[0.102, 0.2)$

Step 3: Repeat the process until the maximum precision of the machine is reached, or all symbols are encoded. To encode the next character "b", we use the "a" interval created before, and zoom into the subinterval "b", and use that for the next step.

Table 3 calculation of new cumulative probability after symbol "b" and "d" has occurred

Symbol	New "b" Interval
a	$[0.102, 0.1216)$
b	$[0.1216, 0.151)$
c	$[0.151, 0.1608)$
d	$[0.1608, 0.2)$

And lastly, the final result is:

Symbol	New "d" Interval
a	$[0.1608, 0.16864)$
b	$[0.16864, 0.1804)$
c	$[0.1804, 0.18432)$
d	$[0.18432, 0.2)$

Step 4: Transmit some number within the latest interval to send the codeword. The number of symbols encoded will be stated in the protocol of the image format, so any number within $[0.1608, 0.2)$ will be acceptable. To decode the message, a similar algorithm is followed, except that the final number is given, and the symbols are decoded sequentially from that order.

3. Results and Discussions

The three experimental works are reported to evaluate the performance of the proposed algorithm. The proposed algorithm was tested on the real images acquired from patients. Each image had a size of 256x256 pixels. All the algorithms were implemented in MATLAB 9.0 on a Pentium IV PC (with CPU 2.8G and 512M memory).

3.1 Quality Measures

The quality of the image or video data [24] to be measured at the output of the decoder, entropy, mean square error (MSE)

and peak to signal to noise ratio (PSNR), time period and compression ratio are often used.

3.1.1 Entropy

An entropy-based cost function is used to measure the compactness of signal (image) representation. The entropy (E) is defined as

$$E = - \sum_{e \in s} p(e) \log_2 p(e) \quad (6)$$

where s is the set of processed coefficients and p (e) is the probability of processed coefficients.

3.1.2 Peak signal noise ratio (PSNR)

The peak signal-to-noise ratio is defined as the ratio between signal variance and reconstruction error variance. MSE is calculated as:

$$MSE = \sigma_q^2 = \frac{1}{M \times N} \sum_{i=1}^M \sum_{j=1}^N [X_{ij} - Y_{ij}]^2 \quad (7)$$

Where the sum over i,j denotes the sum over all pixels in the image and M*N is the number of pixels in each image. X_{ij} - original image, Y_{ij} -Reconstructed image. The PSNR in terms of decibels (dBs) is given by:

$$PSNR = 10 \log_{10} \left(\frac{255^2}{MSE} \right) \quad (8)$$

3.1.3 Time period

The time period is defined as the time taken by each method to undergo compression and decompression stages involved in the algorithm.

3.1.4 Compression ratio

The capability of compression system is characterized by compression ratio which is calculated as

$$\text{Compression Ratio} = \frac{\text{size of the compressed image}}{\text{size of the original image}} \quad (9)$$

The compression ratio values calculated for the set of simulated medical images. Thus it could be seen from the simulated data that the proposed algorithm has the best compression ratio than the existing algorithms. The simulated output of proposed method are discussed below, Fig 9 shows the input medical images for the compression. Fig 10 shows the Edge detected image. Fig 11 shows the Energy mapped image. Fig 12 shows the Retargeted (Resize) image. Fig 13 shows the outputs of the integer wavelet transform of an image and finally fig 14 shows the reconstructed images using the proposed method.

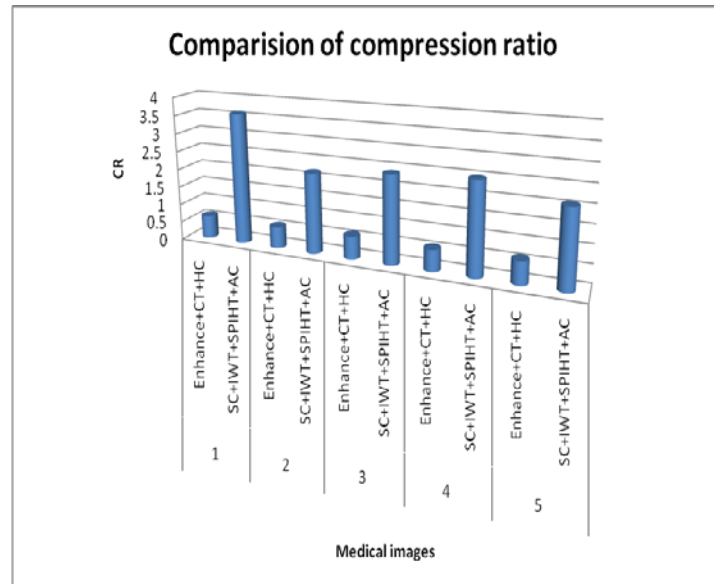


Figure 7: CR value for different medical images using various methods

Table 4: Quality measures for different medical images using proposed method

Medical images	Methods	Time period (Sec)	Entropy (b/s)
1	Enhance+CT+HC	4.45	-
	SC+IWT+SPIHT+AC	5.13	6.1
2	Enhance+CT+HC	4.14	-
	SC+IWT+SPIHT+AC	3.28	7.2
3	Enhance+CT+HC	4.44	-
	SC+IWT+SPIHT+AC	6.77	7.3
4	Enhance+CT+HC	4.34	-
	SC+IWT+SPIHT+AC	6.6	7.5
5	Enhance+CT+HC	4.55	-
	SC+IWT+SPIHT+AC	7.39	7.4

Table 5: PSNR value for Brain medical images using various methodologies

Paper	Methodology	PSNR(dB)
36	BPN	22.5
26	Enhance+CT+HC	12.0
24	SC+WT+SPIHT	45.58
Proposed method	SC+IWT+SPIHT+AC	46.2

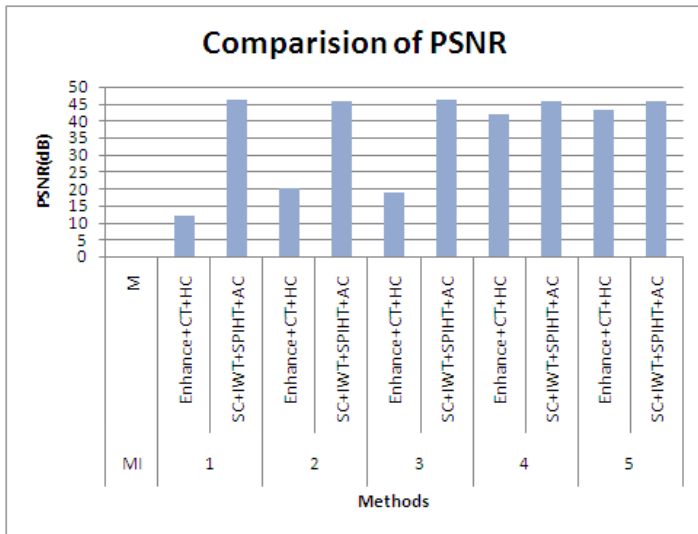


Figure 8: PSNR value for different medical images using various methodologies

It could be observed from the table that the PSNR for different medical images using the proposed method is very high as compared to the existing method [31] and also the time involved is just 7.39 seconds for the proposed algorithm while the existing algorithm takes 17 seconds. Hereby it is concluded that an existing coding[31] takes more time for executing the entire process while the proposed algorithm takes very less time comparatively.

The quality measures such as compression ratio (CR), peak signal to noise ratio (PSNR) are plotted for the existing and the proposed method as shown in Figure 7 – 8. Figure 7 shows the CR for the five input medical images from which it is clearly evident that the CR is greater in the proposed method than the existing method. It is clearly evident from table 5, that the PSNR value is 46.2 dB for the proposed method using the SC+IWT+SPIHT+AC method, while it is around 45 dB for the existing method. This parameter needs to be close to 50dB which is best achieved by the proposed method.

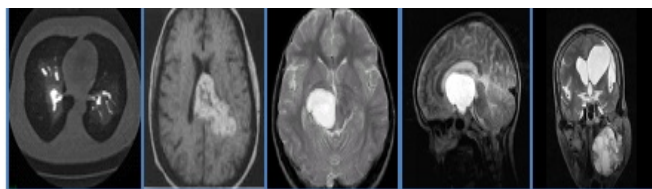


Fig 9: Input medical images

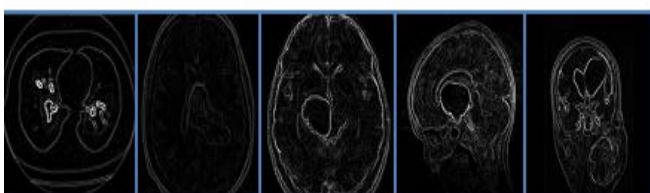


Fig 10: Edge detected image

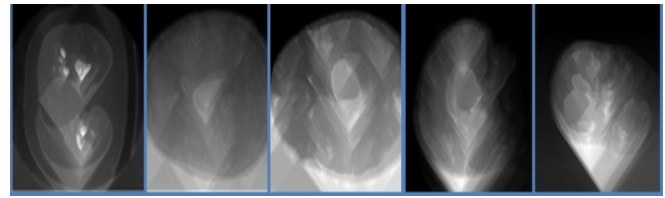


Fig 11: Energy mapped image

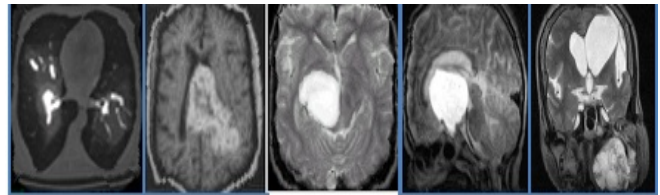


Fig 12: Retargeted (Resize) image

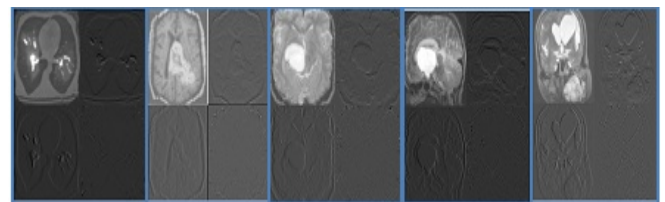


Fig 13: Integer wavelet transform of image

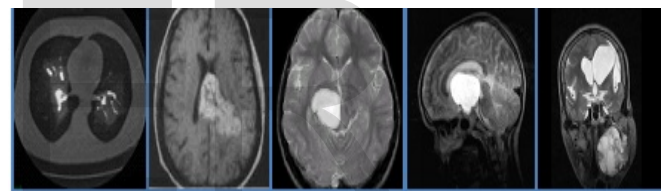


Fig 14: Reconstructed image

4. Conclusion

This method provide better compression ratio with good quality and reduce the processing time based on seam carving technique followed by integer wavelet transform and set partitioning in hierarchical tree, arithmetic coding. Also, the seam carving process was presented to retarget the image corresponding to display set size. Here near lossless embedded coding used to reduce the redundancy, performance was analyzed through determining the image quality after decompression, compression ratio and execution time. This method can be further enhanced by modifying the transformation technique for improving the efficiency of the technique.

REFERENCES

- [1] Sukhwinder Singh, Vinod Kumar, H.K.Verma, "Adaptive threshold based block classification in medical image compression for teleradiology", Computers in Biology and Medicine, Vol.37, pp. 811 – 819,2007

- [2] Rafeef Abugharbieh, Victor Sanchez, and PanosNasiopoulos, "3-D Scalable Medical Image Compression With Optimized Volume of Interest Coding", IEEE Transactions On Medical Imaging, Vol. 29, No. 10, October 2010
- [3] Gregorio Bernab , Jose M. García , José González , "A lossy 3D wavelet transform for high-quality compression of medical video", The Journal of Systems and Software, Vol. 82, pp.526–534,2009
- [4] Yen-Yu Chen, " Medical image compression using DCT-based sub band decomposition and modified SPIHT data organization", International journal of medical informatics, Vol.76, pp. 717–725, 2007
- [5] R. Srikanth, A.G. Ramakrishnan, "Contextual encoding in uniform and adaptive mesh based lossless compression of MR images", IEEE Transactions on Medical Imaging, Vol. 24, pp.1199–1206, 2005.
- [6] R. Shyam Sunder, C. Eswaran, N. Sriraam, "Medical image compression using 3-D Hartley transform", Comput. Biol. Med, Vol.36, pp.958–973, 2006.
- [7] A.T. Deever, S.S. Hemami , "Lossless image compression with projection-based and adaptive reversible integer wavelet transforms", IEEE Transactions on ImageProcessing. vol.12 , pp.489–499. 2003.
- [8] David Wu, Damian M. Tan, Marilyn Baird, John DeCampo, Chris White, and Hong Ren Wu, "Perceptually Lossless Medical Image Coding", IEEE Transactions On Medical Imaging, Vol. 25, No. 3, March 2006
- [9] A. Sivanantha Raja, D. Venugopal and S. Navaneethan, "An Efficient Coloured Medical Image Compression Scheme using Curvelet Transform", European Journal of Scientific Research ISSN 1450-216X Vol.80 No.3 (2012), pp.416-422
- [10] Marykutty Cyriac and Chellamuthu C., "A Novel Visually Lossless Spatial Domain Approach for Medical Image Compression", European Journal of Scientific Research ISSN 1450-216X Vol.71 No.3 (2012), pp. 347-351
- [11] M.Ferni Ukrit ,A.Umameswari ,Dr.G.R.Suresh , —A Survey on Lossless Compression for Medical Images || International Journal of Computer Applications (0975 – 8887) Volume 31– No.8, October 2011
- [12] Aleksej Avramovic and Slavica Savic "Lossless Predictive Compression of Medical Images", Serbian Journal Of Electrical Engineering Vol. 8, No. 1, February 2011, 27-36
- [13]Mrs.S.Sridevi ,Dr.V.R.Vijayakumar and Ms.R.Anuja, "A Survey on Various Compression Methods for Medical Images", IJ. Intelligent Systems and Applications, 2012, 3, 13-19 Published Online April 2012 in MECS
- [14] Balpreet Kaur,Deepak Aggarwal, and Gurpreet Kaur, 4Amandeep Kaur "Efficient Image Compression based on Region of Interest", IJCST Vol. 2, Issue 1, March 2011 ISSN:2229-4333(Print)|ISSN:0976- 8 491
- [15] Pasumpon Pandian, A. and S.N. Sivanandam, "Hybrid Algorithm for Lossless Image Compression using Simple Selective Scan order with Bit Plane Slicing", Journal of Computer Science 8 (8): 1338-1345, 2012 ISSN 1549-3636
- [16] Harjeetpal singh and Sakhi Sharma, "Hybrid Image Compression Using DWT, DCT & Huffman Encoding Techniques", International Journal of Emerging Technology and Advanced Engineering, ISSN 2250-2459, Volume 2, Issue 10, October 2012
- [17] Z. Xiong, X. Wu, S. Cheng, J. Hua, "Lossy to lossless compression of medical volumetric data using 3D integer wavelet transforms", IEEE Transactions on Medical Imaging ,vol.22, pp.459–470, 2003.
- [18] B. Ramakrishnan, N. Sriraam, "Internet transmission of DICOM images with effective low bandwidth utilization", Journal of Digital Signal Process, Vol.16, pp. 825–831,2006.
- [19] N. Sriraam, R. Shyamsunder." 3-D medical image compression using 3-D wavelet coders", Elsevier on Digital Image Processing,Vol.21,pp.100-109,2010.
- [20] Janaki. R and Dr.Tamilarasi, "A,Still Image Compression by Combining EZW Encoding with Huffman Encoder", International Journal of Computer Applications (0975 – 8887) Volume 13– No.7, January 2011
- [21] Avidan S. and Shamir A.'A seam carving for content-aware image resizing' (2007) ACM Trans. Graphics, vol. 26, no. 3, pp. 10–19.
- [22] Gutierrez D Rubinstein.M Shamir and A. Sorkine O.(2010) 'A comparative study of image retargeting 'ACM Trans. Graphics, vol. 29, no. 6,pp. 160–168
- [23] Hasegawa M Kato S. and Tanaka Y. (2010) 'Image coding using concentration and dilution based on seam carving with hierarchical search' in Proc. IEEE Int. Conf.Acoust., Speech. Signal Process.pp. 1322–1325
- [24] E.Salma,J.P. Josh Kumar , 'Efficient Image Compression based on Seam Carving for Arbitrary Resolution Display Devices', International Journal of Computer Applications Volume 68– No.4, April 2013.pp.37-40
- [25] M. Moorthi, R. Amutha , "Medical Image Compression using Contourlet with SVD Transform and Huffman coder", 2013, viruksha Journal.(Article in press)
- [26] Heikkila M., Pietikainen M. and Heikkila J., "A Texture-Based Method for Detecting Moving Objects," The 15th British Machine Vision Conference I: pp. 187-196, 2004.
- [27] Turtinen M. and Pietikainen M., "Visual Training and Classification of Textured Scene Images," 3rd International Workshop on Texture Analysis and Synthesis pp. 101-106, 2003.
- [28] Ojala T., Pietikainen M., Maenpaa T., "Multiresolution Gray-Scale and

Rotation Invariant Texture Classification with Local Binary Patterns," IEEE Transactions on Pattern Analysis and Machine Intelligence 24 pp. 971-987, 2002.

[29] Ramana Reddy B.V., Radhika Mani M. Sujatha B., Vijaya Kumar V., "Texture Classification Based on Random Threshold Vector Technique," International Journal of Multimedia and Ubiquitous Engineering Vol. 5, No. 1, January, 2010

[30] Mikael Rousson, Nikos Paragios, and Rachid Deriche. Implicit active shape models for 3d segmentation in mr imaging. *Medical Image Computing and Computer-Assisted Intervention – MICCAI 2004*, pages 209–216, 2004.

[31] Daniel Cremers, Mikael Rousson, and Rachid Deriche. A review of statistical approaches to level set segmentation: Integrating color, texture, motion and shape. *Int. J. Comput. Vision*, 72(2):195–215, 2007.

[32] Rosin, P. Training Cellular Automata for Image Processing. *IEEE Transactions on Image Processing*, Vol. 15, No. 7, pp. 2076-2087. (2006).

[33] Cheng, H. D., Shi, X.J., Min, R., Hu, L.M., Cai, X.P. & Du, H.N. Approaches for Automated Detection and Classification of Masses in Mammograms. *Pattern Recognition*, Vol. 39, pp. 646-668, (2006).

[34] Wongthanavas, S. & Tangvoraphongchai, V. CA-based Algorithms and Its Application in Medical Image Processing. *Proceedings of ICIP 2007 14th International Conference on Image Processing*, pp. III-41-44, ISBN: 1-4244-1437-7, ISSN: 1522-4880, San Antonio, Texas, U.S.A. September 16-19, 2007.

[35] Chen, J.-C., Yeh, C.-M. & Tzeng, J.-E. Pattern differentiation of glandular cancerous cells and normal cells with cellular automata and evolutionary learning. *Expert Systems with Applications*, Vol. 34, Issue 1, , pp. 337-346, 2008

[36] M. Moorthi, R. Amutha, " Medical Image Compression using Adaptive Neural Network", *IEEE-International Conference on Emerging Trends in Science, Engineering and Technology (INCOSSET)*, pp 222- 227, 2012.

He has published and presented papers in National and International Conference in the area of Image processing. He has been the reviewer for 2012 & 2013 IET image processing. His research interests are Image Segmentation, Image Compression, Neural network, Fuzzy logic, microprocessor and micro-controller.



Dr. R. Amutha, Professor, ECE department graduated from Thiagarajar college of Engineering in the year 1987. She obtained her M.E degree from PSG college of Technology. She got her Ph.D from Anna University in 2006. She has 24 years of teaching and 10 years research experience. Her research area includes coding theory, Wireless communication network and Image processing. She published 3 International and 2 national journal papers. She has 20 International and national conference papers to her credit. She reviewed three international journal papers. She is a recognized research supervisor of Anna University and SCSVMV University for Ph.D and M.S (by research). She is supervising 9 Ph.D research scholars.



M. Moorthi pursuing his Ph.D program at Sri Chandrasekharendra Saraswathi Viswa Mahavidyalaya University, Kanchipuram. He completed his B.E degree at Arulmigu Meenakshi Amman College of Engineering, Kanchipuram, in Electronics and Communication Engineering in the year 2001 and M.E - Medical Electronics in the year 2007 at Anna University, Gundy campus, Chennai, India. He has 12 years of teaching experience and he is currently working as Assistant Professor in the department of Electronics and Communication Engineering at Prathyusha Institute of Technology and management, Chennai. He is a member of the Institute of Electrical and Electronics Engineers (IEEE), Indian Society for Technical Education (ISTE), IETE.